Supporting Information for

Acid-Induced Structural Regulation of Spiropyran-Modified Mixed Matrix Membranes for Enhanced CO_2/CH_4 Separation

Zhiqing Xu,[‡a] Yaxu He,[‡a] Qiujian Xie,[a] Yufei Liu,[a] Qianpan Guo,[a] Chunyue Pan,[a] Shuai Gu,*[ab] Juntao Tang,*[a] Guipeng Yu*[a]

[a] *Hunan Key Laboratory of Micro & Nano Materials Interface Science, College of Chemistry and Chemical Engineering, Central South University, Changsha, 410083, China*

[b] *Key Laboratory of Advanced Energy Materials Chemistry (Ministry of Education), Nankai University, Tianjin 300071, P. R. China.*

[‡] These authors contributed equally.

Table of contents

Section A. Experimental Section

1. Materials

2,3,3-Trimethyl-5-bromo-3H-indole, chloroform-*d*, acetone-d_6, DMSO-d_6, TFA, and TEA were all ordered from Sahn Chemical Technology (Shanghai) Co., LTD. Iodomethane was ordered from Yanfeng Technology (Beijing) Co., LTD. tris(dibenzylideneacetone) dipalladium, 5-Bromosalicylaldehyde, 1,4-benzenediboronic acid bis(pinacol) ester, 2-dicyclohexylphosphino-2′,6′-dimethoxybiphenyl (SPhos), and Methyltrioctylammonium chloride (Aliquat 336) were all ordered from Shanghai Titan Technology Co., LTD.

2. Synthesis

2.1 Synthesis of DBr-TMNS

2,3,3-Trimethyl-5-bromo-3H-indole (1.2 g, 5 mmol) was added to a 50 mL two-mouth round-bottom flask, then 25 mL acetonitrile and 0.6 mL iodomethane were added, and reflux was carried out overnight under nitrogen protection. After the reaction was completed, the crude product was added to 500 mL two-orifice round-bottom flask, and 40 wt% sodium hydroxide (150 mL) and ether (50 mL) were mixed into the flask, and stirred at room temperature for 4 h under N_2 atmosphere. After the reaction, the organic phase was separated, washed with water (2×50 mL), dried with anhydrous sodium sulfate, pumped and filtered, and then steamed to obtain red oil. The crude oil [SiO_2, dichloromethane (DCM)/cyclohexane (CYH) (7:3, v/v)] was purified by column chromatography to obtain 5-bromo-1,3,3-trimethyl-2-methylene indole. Then 5-Bromosalicylaldehyde (1.1 g, 0.6 mmol) and 5-bromo-1,3,3-trimethyl-2-methylene indole (1.3 g, 0.5 mmol) were added to 150 mL of n-propanol (NPA) and stirred, and reflux for 36 h under N_2 protection. At the end of the reaction, the crude product was distilled and concentrated under reduced pressure, and the crude solid was precipitated from ethanol to separate the DBr-TMNS. ^{1}H NMR (400 MHz, Acetone-d_6, δ, ppm): 7.36 (d, J = 2.4 Hz, 1H), 7.28 (dd, J = 4.7, 2.3 Hz, 1H), 7.26 (dd, J = 5.0, 2.2 Hz, 1H), 7.24 (d, J = 2.0 Hz, 1H), 7.03 (d, J = 10.3 Hz, 1H), 6.65 (d, J = 8.6 Hz, 1H), 6.55 (d, J = 8.2 Hz, 1H), 5.87 (d, J = 10.3 Hz, 1H), 2.72 (s, 3H), 1.29 (s, 3H), 1.18 (s, 3H).

2.2 Synthesis of TSP-1 polymer

DBr-TMNS (0.5 g, 1.1 mmol), 1,4-Benzenediboronic acid bis(pinacol) ester (0.4 g, 1.1 mmol), $Pd_2(dba)_3$ (0.01 g, 0.01 mmol) and Sphos (0.02 g, 0.03 mmol) was added with 2 drops of Aliquat 336, K_2CO_3 aqueous solution (1 mL, 2 M) and toluene (2 mL). Purge and degas with nitrogen and stir at 80 ℃ for 72 h. After cooling, the organic phase was washed with saturated NaCl solution and water until the wash solution becomes neutral (Remove K_2CO_3, Pd catalyst and other water-soluble by-products). The organic phase was dropped into methanol (500 mL) to precipitate the solid (Remove unreacted 1,4-benzenediboronic ester, DBr-TMNS and Aliquat 336). The precipitation was dissolved in tetrahydrofuran (THF) (150 mL), and then the solution was dropped into methanol (700 mL) (further purification) to obtain about 0.4 g of TSP-1 polymer with a yield of 90.5%. The molecular weight of polymer TSP-1 was determined using gel permeation chromatography (GPC), with a number-average molecular weight (M_n) of 14,111 g/mol and a weight-average molecular weight (M_w) of 45,558 g/mol (Table S2).

2.3 Preparation of TSP-1/PIM-1 mixed matrix membranes

TSP-1/PIM-1 mixed matrix membranes with 8 wt% were prepared by solution casting method. Weigh a total of 200 mg PIM-1 powder and TSP-1 powder and add 3 mL chloroform solution. Stir for 12 h until a uniform TSP-1/PIM-1 solution is formed. The prepared casting liquid was cast on a flat petri dish and the solvent volatilized at room temperature to obtain the mixed matrix membrane.

2.4 Preparation of TMC-1/PIM-1 mixed matrix membranes

TMC-1/PIM-1 mixed matrix membranes were obtained by treating the prepared TSP-1/PIM-1 mixed membrane with a methanol solution containing 75% TFA.

3. Characterizations

The molecular structure simulation and optimization of TSP-1 polymer were performed using Gaussian software to determine the optimal conformation of the polymer chains and their dihedral angles, as well as to analyze the intramolecular non-covalent interactions within the polymer. The specific steps are as follows: The monomer unit of the TSP-1 polymer was drawn in Materials Studio (MS) software, saved, and then

loaded into GaussView software. The monomer unit was duplicated and the end groups of the unit structures were connected according to the condensation reaction process to form a polymer molecular chain structure containing three spiropyran units. Due to the large molar mass of the repeating unit of the TSP-1 polymer, the short-chain structure used for calculation only contains two repeating units. The “Clean” button was clicked to perform an initial optimization of the polymer structure. The “Calculate” button was clicked to set the Gaussian calculation parameters. The “DFT” functional was selected and the calculation was submitted, which was carried out in the Gaussian software. The non-covalent interactions between polymer molecular chains were mainly analyzed using the Multiwfn quantification program and visualized using the VMD program. The specific steps are as follows: The spiropyran molecules in the molecular chain and the surrounding atoms were defined as two separate fragments for Independent Gradient Model of Hirshfeld (IGMH) analysis. The Multiwfn quantification program was launched and the analysis parameters were set for non-covalent interactions. After the calculation was completed, the grid data was exported in the “cub” file format. The VMD program was then launched and the relevant parameters were set to export the non-covalent interaction analysis diagram. The strength of the non-covalent interactions between the atoms of the molecular chain was analyzed based on the green surface in the diagram. The molecular free volume fraction of the polymer was calculated using the molecular simulation method in MS software. The steps for the simulation calculation of free volume are as follows: The repeating unit structure of the polymer to be calculated was drawn in MS software. Several repeating units were connected to form a short polymer chain, which served as the basic chain. For TSP-1 and PIM-1, the basic chain consisted of 10 repeating units. A cubic grid for the simulation calculation of the amorphous polymer was created, with the initial number of basic chains inside the cubic grid set to 6. The multiple basic chains within the created cubic grid were observed. Based on the proximity principle, two end groups belonging to two different basic chains were selected and connected, followed by hydrogen atom filling, potential energy minimization, geometric optimization, and simulated annealing (NPT mode) operations. This was done to further extend the length

of the polymer main chain, increase the molecular weight to approach a realistic state. The operation in the previous step was repeated five times until only one polymer chain remained, i.e., two end groups were left. Then, the obtained polymer model was subjected to thorough geometric optimization and annealing (NVT mode). At the same time, the density within the cubic grid reached a stable state, meaning that the polymer structure within the cubic grid achieved a uniform distribution without significant voids. The parameters were set (probe size set to 0.33 nm, simulating the molecular dynamics diameter of CO_2) to simulate the dynamic state of the polymer long chain within the cubic grid. After the calculation was completed, the generated dynamic structure file was double-clicked. The free volume fraction was calculated based on a certain frame state, with the free volume fraction being equal to the free volume divided by the volume occupied by the polymer.

The molecular structure changes of polymer and polymer membrane before and after discolouring were characterized by Fourier transform infrared spectrometer (FTIR). The test instrument model was Rayleigh WQF-510A, and the sample preparation method was potassium bromide tablet. The molecular structure of monomers and polymers was characterized by liquid nuclear magnetic resonance (^{1}H and ^{13}C). The test instrument model was Bruker Advance III 400 MHz NMR instrument, and the test temperature was room temperature. Acetone-d_6, $CDCl_3$, or DMSO-d_6 with tetramethylsilane (TMS) as the internal target were used as solvents. The specific surface area and pore size distribution of TSP-1 polymer and TSP-1/PIM-1 blend were characterized by specific surface and pore size analyzer, and the changes of CO_2 adsorption properties of TSP-1 polymer and TSP-1 blend membrane at 273 K and 298 K before and after acid action were tested. The test instrument model was Jingwei Gaobo JW-BK132F. Nitrogen adsorption and desorption experiments were carried out at 77 K, and the pore size distribution of the polymer was calculated and analyzed by NLDFT method using non-local density functional theory. Before the test, the sample was degassed under vacuum at 100 ℃ for more than 12 h. Scanning electron microscopy (SEM) was used to characterize the surface morphology of the polymer membrane. The test instrument model was JSM-7610FPlus. Before the test, the sample

was dispersed on the conductive membrane attached to the copper sample holder, and then gold was sprayed by sputtering machine (30 mA current, 120 s sputtering at vacuum room temperature). The molecular weight of the polymer was characterized by gel permeation chromatography. The test instrument model was Agilent 1260 Infinity II, the mobile phase was chromatocl-grade tetrahydrofuran, and the test temperature was room temperature. The thermogravimetric instrument was used to characterize the thermal stability of the polymer. The test instrument model was TGA 2 SF/1100, the nitrogen flow rate was 50 mL/min, the heating rate was 10 ℃/min, and the test temperature was 100-800 ℃. UV visible spectrometer was used to characterize the light absorption of polymer before and after discoloration in solution. The test instrument model was UV 8100 A and the wavelength range was 200-700 nm. The UV-Visible light absorption wavelength of the blended membrane was measured by UV-Visible-near-infrared diffuse reflectometer (Shimadzu UV-3600, Japan). The molecular structure of TSP polymer was simulated and optimized by Gauss, the optimal conformation and dihedral Angle of the molecular chain were determined, and the intramolecular non-covalent forces of the polymer were analyzed. The non-covalent interaction between polymer molecular chains was analyzed by Multiwfn quantization program and visualized by VMD program. Molecular simulation method was used to calculate the molecular free volume fraction of the polymer on the Material studio (MS) software. The hydrophilicity of the polymer membrane was tested by a contact Angle measuring instrument, model JC2000D1. Universal testing machine was used to test the elongation at break and the maximum tensile strength of polymer membrane (length * width * height =25 mm * 5 mm * 0.06 mm). The test instrument model was American INSTRON 68TM^{-5}, the pressure sensor was 1 KN, the tensile rate was 1 mm/min, and the test temperature was 30℃. The relative humidity is 30-50%. A differential scanning calorimeter was used to characterize the glass transition temperature of the polymer membrane. The test instrument model was DSC 3/700, the nitrogen flow rate was 50 mL/min, the heating rate was 10 ℃/min, and the test temperature was 25-500℃.

Wicke-Kallenbach technology was used to test the gas separation performance of the membrane on a self-lap gas permeation device, and gas chromatography (Agilent GC

8860) was used to achieve online detection of gas components. The gas flow rate of single-component gas permeation at the feed side was 50 mL/min. The total gas flow on the feed side of the two-component gas permeation was 100 mL/min, the flow rate of the two gases was 50 mL/min, the flow rate of the purge gas on the permeation side was 15 mL/min, the test temperature was room temperature, and the pressure difference on both sides of the membrane was 0.2 MPa. Permeability (P: Barrer) and selectivity (α) were used to evaluate the performance of gas separation membranes.

$$P = D \times S = 10^{10} \times \frac{V_d \times l}{P_{up} \times T \times R \times A} \times \frac{dp}{dt}$$

$$a_{i,j} = P_i / P_j$$

$$\alpha_{i,j} = \frac{x_{i,permeate} / x_{j,permeate}}{x_{i,feed} / b_{j,feed}}$$

$$D = l^2 / 6\Theta$$

$$S = P / D$$

Where, Permeability (P): Barrer, 1 Barrer = 10^{-10} cm^3 (STP) cm cm^{-2} s^{-1} $cmHg^{-1,}$ Diffusion coefficient (D): 10^{-8} cm^2 s^{-1}, Solubility coefficient (S): 10^{-2} cm^3 (STP)/cm^3·cmHg, Rated penetration volume (V_d): cm^3, membrane thickness (l): cm, Upstream pressure (P_{up}): cmHg, Operating temperature (T): K, Gas constant (R): 0.278 cm^3 cmHg cm^{-3} (STP) K^{-1}, Membrane area (A): cm^2, Steady downstream pressure increment (dp/dt): cmHg s^{-1}, x_i, feed represents the concentration of gas i on the feeding side (%), x_j, feed represents the concentration of gas j on the feeding side (%), x_i, permeate represents the concentration of gas i on the permeating side (%), x_j, permeate represents the concentration of gas j on the permeating side (%), Residence time (θ): s.

Section B. Supporting Figures

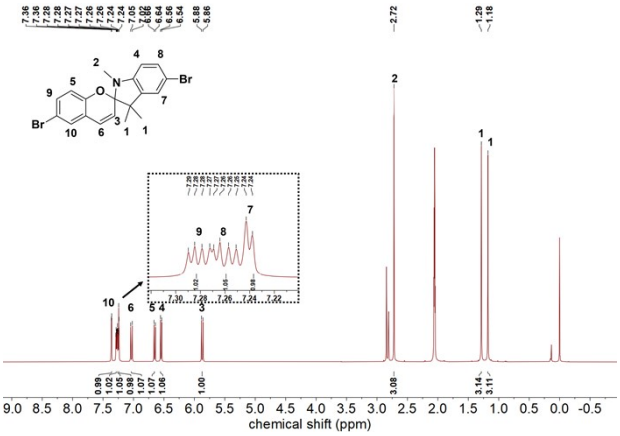

Fig. S1 ^{1}H NMR spectrum of DBr-TMNS (400 MHz, $(CD_3)_2CO$ -d_6).

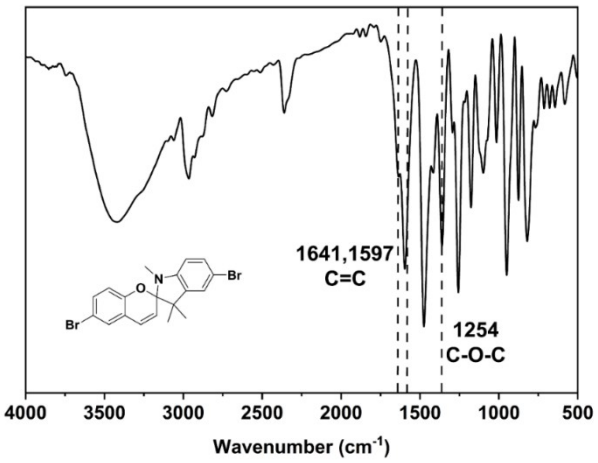

Fig. S2 FTIR spectrum of DBr-TMNS.

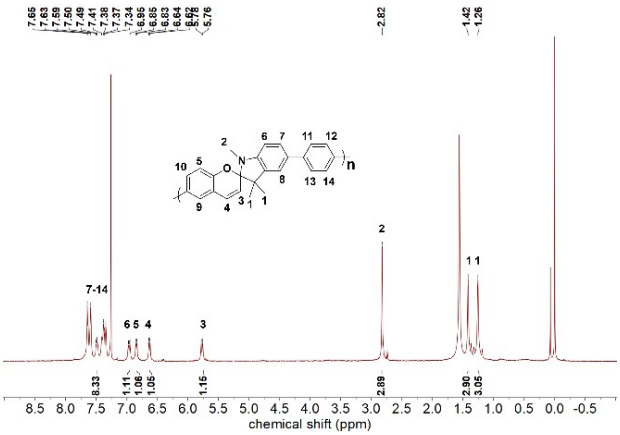

Fig. S3 ^{1}H NMR spectrum of TSP-1 (400 MHz, $CDCl_3$).

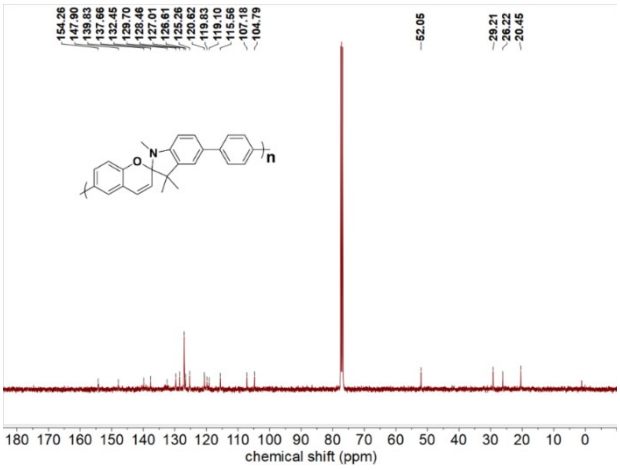

Fig. S4 ^{13}C NMR spectrum of TSP-1 (400 MHz, $CDCl_3$).

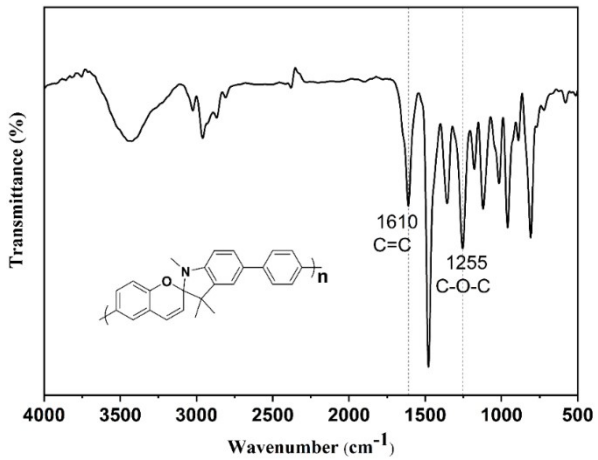

Fig. S5 FTIR spectrum of TSP-1.

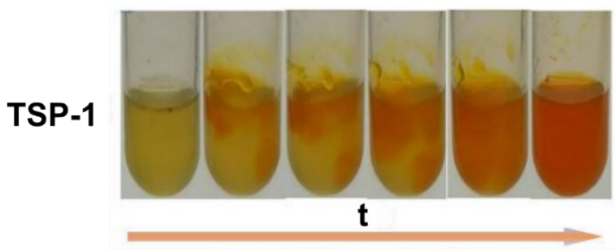

Fig. S6 Optical microscopy images of the TSP-1 chloroform solution over time after the addition of TFA.

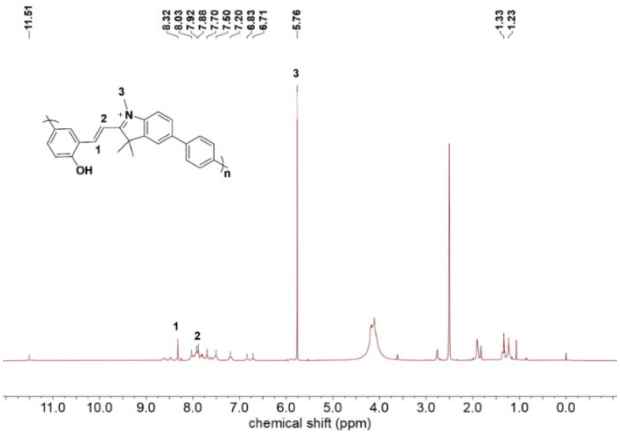

Fig. S7 ^{1}H NMR spectrum of TMC-1 (400 MHz, DMSO-d_6).

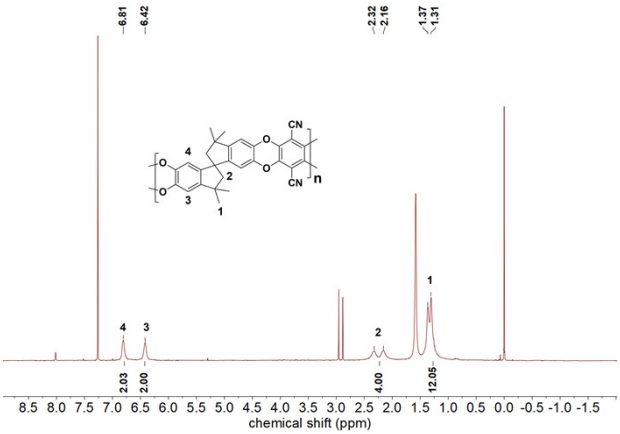

Fig. S8 ^{1}H NMR spectrum of PIM-1 (400 MHz, $CDCl_3$).

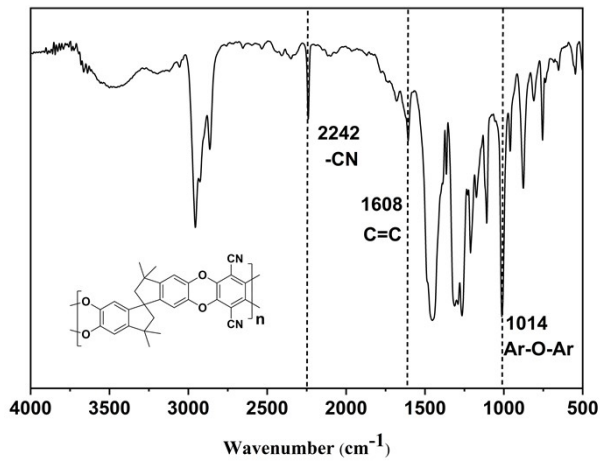

Fig. S9 FTIR spectrum of PIM-1.

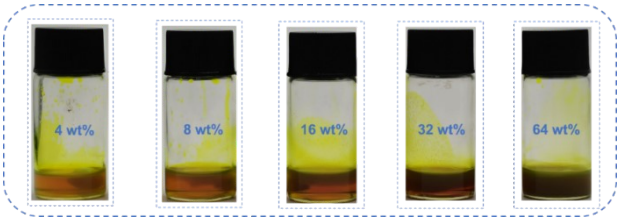

Fig. S10 The solution blending experiment with different loading capacities of TSP-1 and PIM-1.

With the increase in the incorporation amount of TSP-1, the solution gradually becomes turbid, indicating that there is a certain threshold for the compatibility between TSP-1 and PIM-1. When the loading amount of TSP-1 exceeds a certain value (>16 wt%), the compatibility between the filler and the matrix decreases, potentially leading to phase separation or filler agglomeration, thereby affecting the uniformity and performance of the material.

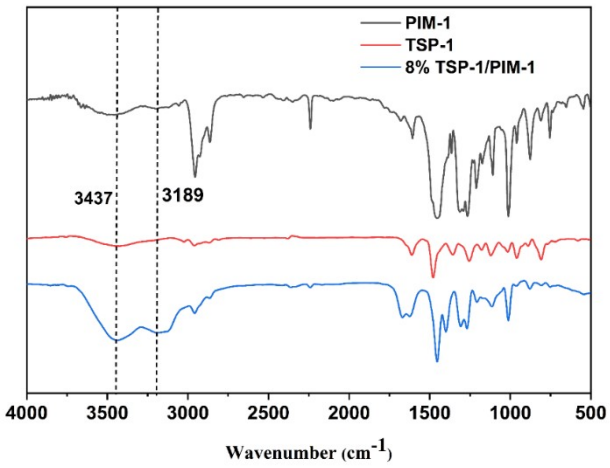

Fig. S11 FTIR spectrum of TSP-1, PIM-1 and 8 wt% TSP-1/PIM-1.

At 3440 cm^{-1} and 3189 cm^{-1}, no distinct hydrogen bonding characteristic peaks were observed for either PIM-1 or TSP-1. However, a broad hydrogen bonding characteristic peak emerged in the 8wt% TSP-1/PIM-1 blend. This suggests that hydrogen bonds, a type of non-covalent interaction, may have formed between TSP-1 and PIM-1, thereby accounting for the good compatibility observed between the two materials.

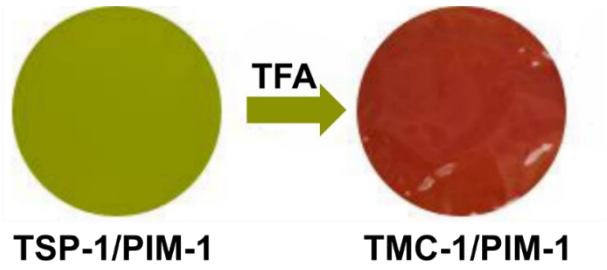

Fig. S12 Optical microscopy images of the membrane before and after acid treatment.

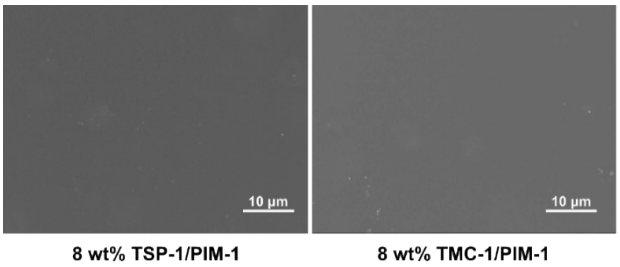

Fig. S13 SEM images of 8 wt% TSP-1/PIM-1 and 8 wt% TMC-1/PIM-1.

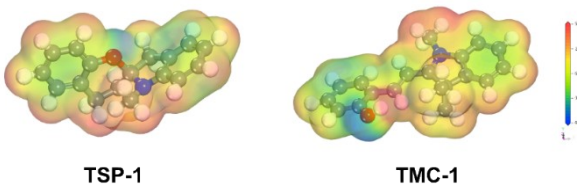

Fig. S14 Calculated electron cloud density maps of TSP-1 and TMC-1 fragments.

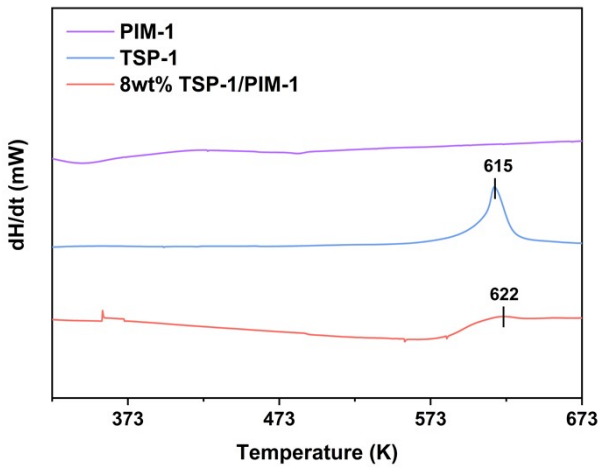

Fig. S15 DSC analysis of TSP-1, PIM-1 and TSP-1/PIM-1.

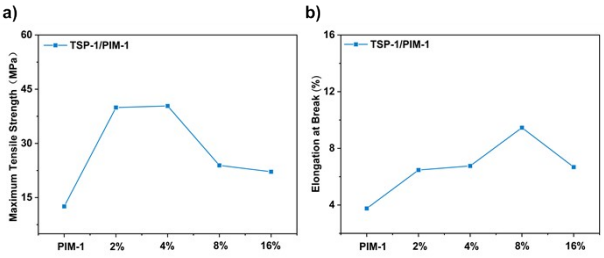

Fig. S16 a, b) Maximum Tensile Strength and Elongation at break of 0-16wt% TSP-1/PIM-1.

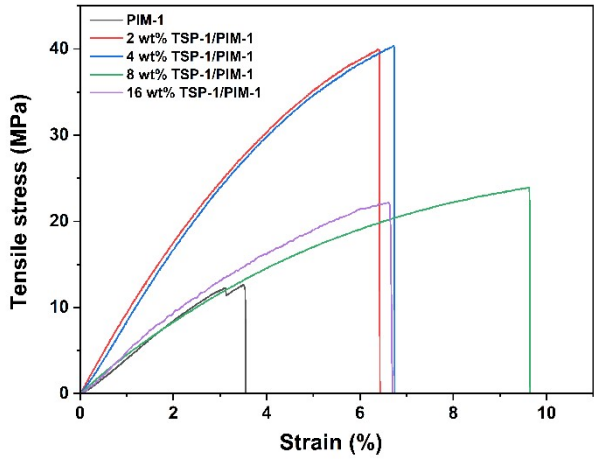

Fig. S17 Stress–strain curve of 0-16wt% TSP-1/PIM-1.

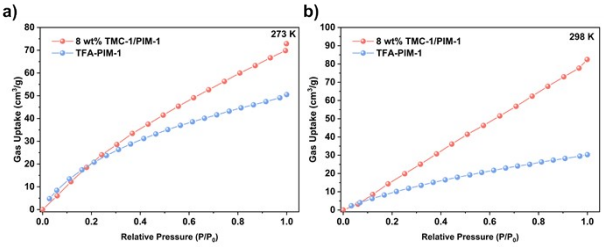

Fig. S18 a, b) CO_2 adsorption isotherms of acid-treated PIM-1 and 8 wt% TMC-1/PIM-1 under 273K and 298K.

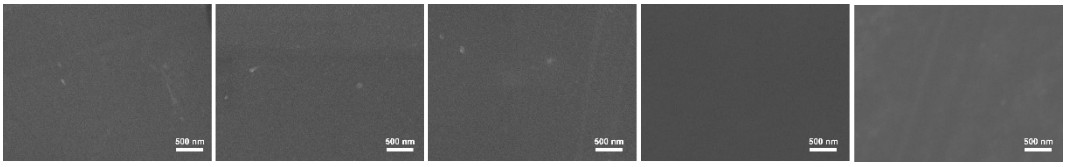

Fig. S19 SEM images of 0, 2, 4, 8 and 16 wt% TSP-1/PIM-1.

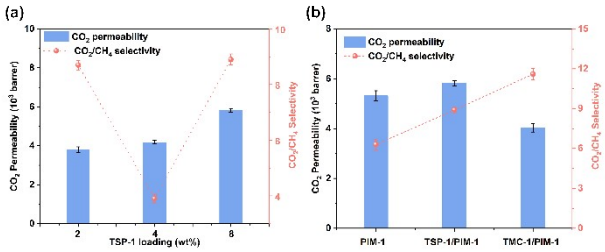

Fig. S20 (a) Mixed-gas CO_2 permeability and CO_2/CH_4 selectivity graphs of 2, 4 and 8 wt% TSP-1/PIM-1. (b) Mixed-gas CO_2 permeability and CO_2/CH_4 selectivity graphs of PIM-1, 8 wt% TSP-1/PIM-1 and 8 wt% TMC-1/PIM-1.

Fig. S21 Optical microscopy images of 0, 2, 4, 8 and 16 wt% TSP-1/PIM-1.

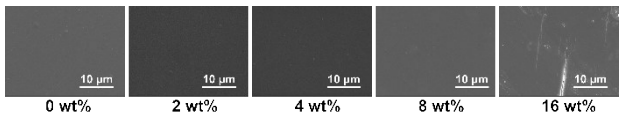

Fig. S22 SEM images of 0, 2, 4, 8 and 16 wt% TSP-1/PIM-1.

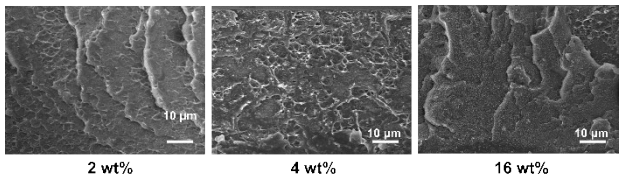

Fig. S23 Cross-sectional SEM images of 2, 4 and 16 wt% TSP-1/PIM-1.

Table S1 CO_2/CH_4 Separation Performance Data of PIM-1 based MMMs

MMMs	Mass Fraction (wt%)	P_{CO2} (Barrer)	α (CO_2/CH_4)
TSP-1/PIM-1 (this work)	**2**	**5668**	**10.3**
TSP-1/PIM-1 (this work)	**4**	**6514**	**13.3**
TSP-1/PIM-1 (this work)	**8**	**7696**	**18.4**
TMC-1/PIM-1 (this work)	**8**	**13659**	**36.5**
PIM-Py-Ac-15[3]	**15**	**6205**	**56.1**
PAO-PIM-1/NH2-UiO-66[4]	**30**	**8425**	**23**
PIM-30ZIF[1]	**30**	**8377**	**11.2**
PIM-1/P-NP[2]	**30**	**10520**	**13.7**
PIM-1/SNW-1[5]	**10**	**7553**	**13.5**

Table S2 Molecular weight of TSP-1

	M_n (g/mol)	M_w (g/mol)	M_w/M_n	n
TSP-1	**14111**	**45558**	**3.2**	**40**

Section C. Reference

1 L. Hao, K.-S. Liao and T.-S. Chung, *J. Mater. Chem. A*, 2015, **3**, 17273.

2 Y. Kudo, H. Mikami, M. Tanaka, T. Isaji, K. Odaka, M. Yamato and H. Kawakami, *J. Membr. Sci.*, 2020, **597**, 117627.

3 C. Wang, F. Guo, H. Li, J. Xu, J. Hu, H. Liu and M. Wang, *J. Membr. Sci.*, 2020, **598**, 117677.

4 Z. Wang, H. Ren, S. Zhang, F. Zhang and J. Jin, *J. Mater. Chem. A*, 2017, **5**, 10968.

5 X. Wu, Z. Tian, S. Wang, D. Peng, L. Yang, Y. Wu, Q. Xin, H. Wu and Z. Jiang, *J. Membr. Sci.*, 2017, **528**, 273.